Supporting Information

Anionic chalcogen functionalized pentaphosphaferrocene complexes

David Konieczny,[a] Mehdi Elsayed Moussa,[a] Eric Mädl,[a] Stephan Reichl,[a] Mikhail Butovskiy,[a] Michael Bodensteiner,[a] Alexander. V. Virovets[b] and Manfred Scheer[a]*

Department of Inorganic Chemistry, University of Regensburg, GER-93040 Regensburg (Germany)
E-mail: manfred.scheer@chemie.ur.de
Institut für Anorganische und Analytische Chemie, Goethe-Universität Frankfurt am Main, D-60438 Frankfurt am Main (Germany),

Table of Contents:

1. Experimental Details:

1.1 General remarks:

All manipulations were performed under an atmosphere of dry argon using standard glovebox and Schlenk techniques. All solvents were taken from a solvent purification system of the type MB-SPS-800 from the company MBRAUN (Garching, Germany), and degassed by standard procedures. Deuterated solvents were degassed, dried and distilled prior to use. The starting materials were purchased from commercial suppliers: S, Se, KOH, DME, Me_3NO, Na and K (Sigma-Aldrich Chemie GmbH); KH, Ph_3PO, 15crown5, 18crown6 (Merck Chemicals GmbH).
The compounds $[Cp^*Fe(\eta^5\text{-}P_5)]$[1] (**A**), $[K_2(DME)_2][Cp^*Fe(\eta^4\text{-}P_5)]$[2] ($[K_2(DME)_2][$**B**$]$) and $[K_2(DME)_3][Cp^*Fe(\eta^4\text{-}P_5)_2]$[2] ($[K_2(DME)_3][$**C**$]$) were prepared according to literature procedures.
All nuclear magnetic resonance (NMR) spectra were recorded on a Bruker Avance 400 spectrometer (Brucker Instruments, Ettlingen, Germany) (^{1}H: 400.13 MHz, ^{31}P:161.976 MHz, ^{13}C{^{1}H}: 100.623 MHz) with δ [ppm] referenced to external $SiMe_4$ (^{1}H, ^{13}C), H_3PO4 (^{31}P) and $Se(CH_3)_2$ for ^{77}Se. Mass spectra were recorded on a a ThermoQuest Finnigan TSG 7000 mass spectrometer. The C, H, N analyses were measured on an Elementar Vario EL III apparatus.

1.2 Synthesis and characterization of $[K_2(DME)_2]$[1], [1] = $[Cp^*Fe(\eta^4\text{-}P_5S)]^{2-}$:

To a solution of $[K_2(DME)_2][$**B**$]$ (150 mg, 0.25 mmol) in DME (15 mL) at -60°C a solution of sulfur (8.0 mg, 0.25 mmol) in DME (5 mL) was added. The color of the reaction mixture turned from dark olive green to dark brown while slowly warming up to ambient temperature and was stirred for further 18 h at room temperature. The volume of the solution was reduced to ca. 5 mL and layered with *n*-hexane (15 ml). After 2 days at 0°C dark brown microcrystalline precipitate of $[K_2(DME)_2][$**1**$]$ was formed.

Yield:	140 mg (88%).
^{1}H NMR ($THF\text{-}d_8$):	δ [ppm] = 1.39 (s, 15 H, $C_5(CH_3)_5$), 3.28 (s, 12 H, CH_3, DME), 3.43 (s, 8 H, CH_2, DME).
^{13}C{^{1}H} NMR ($THF\text{-}d_8$):	δ [ppm] = 11.4 (s, $C_5(CH_3)_5$), 58.7 (s, CH_3, DME), 72.6 (s, CH_2, DME), 86.1 (s, $C_5(CH_3)_5$).
^{31}P NMR ($THF\text{-}d_8$):	δ [ppm] = 14.6 (m, 2 P), 33.9 (m, 2 P), 107.7 (tt, 1 P).
^{31}P{^{1}H} NMR ($THF\text{-}d_8$):	δ [ppm] = 14.6 (m, 2 P), 33.9 (m, 2 P), 107.7 (tt, 1 P).
ES-MS (THF):	*m/z*: 314.8 (20) $[Cp^*FeP_4H]^-$, 346.7 (37) $[Cp^*FeP_5H]^-$, 378.8 (5) $[Cp^*FeP_5SH]^-$, 408.8 (100) $[C_{10}H_{14}FeP_5S_2]^-$, 417.8 (23) $[C_{10}H_{15}FeP_5SK]^-$.
EA:	calculated for $C_{10}H_{15}FeK_2P_5S$ • 1.5 $C_4H_{10}O_2$: C: 32.50%, H: 5.11%, S: 5.42%; found: C: 32.05%, H: 4.96%, S: 4.67%.

1.3 Synthesis and characterization of $[K_2(DME)_2]$[2], [2] = $[Cp^*Fe(\eta^4\text{-}P_5Se)]^{2-}$:

To a solution of $[K_2(DME)_2][$**B**$]$ (90 mg, 0.15 mmol) in DME (20 mL) at -60°C, a suspension of selenium (11.8 mg, 0.15 mmol) in DME (5 mL) was added. The color of the reaction mixture turned from dark olive green to dark brown while slowly warming up to ambient temperature and was stirred for further 18 h at room temperature. The volume of the solution was reduced to ca. 5 mL and layered with *n*-hexane (15 ml). After 2 days at 0°C dark brown crystals of $[K_2(DME)_2][$**2**$]$ were formed.

Yield:	88 mg (90%).
^{1}H NMR (THF-d_8):	δ [ppm] = 1.38 (s, 15 H, $C_5(CH_3)_5$), 3.28 (s, 6 H, CH_3, DME), 3.43 (s, 4 H, CH_2, DME).
^{13}C{^{1}H} NMR (THF-d_8):	δ [ppm] = 11.5 (s, $C_5(CH_3)_5$), 58.9 (s, CH_3, DME), 72.7 (s, CH_2, DME), 86.3 (s, $C_5(CH_3)_5$).
^{31}P NMR (THF-d_8):	δ [ppm] = 14.5 (m, 2 P), 33.1 (m, 2 P), 81.9 (tt, 1 P).
^{31}P{^{1}H} NMR (THF-d_8):	δ [ppm] = 14.5 (m, 2 P), 33.1 (m, 2 P), 81.9 (tt, 1 P).
^{77}Se NMR (THF-d_8):	δ [ppm] = 352.0 (d, $^{1}J_{(Se,P)}$ = 300 Hz, 1 Se, P*Se*).
ES-MS (THF):	*m/z*: 508.0 (10) $[C_{10}H_{15}FeP_5SK]^-$.
EA:	calculated for $C_{10}H_{15}FeK_2P_5Se \bullet 1.3\ C_4H_{10}O_2$: C: 29.43%, H: 4.55%; found: C: 29.62%, H: 4.13%.

1.4 Synthesis and characterization of $[K_2(THF)_2][3]$, $[3] = [Cp^*Fe(\eta^4\text{-}P_5S_2)]^{2-}$:

To a solution of $[K_2(DME)_3]$[**C**] (250 mg, 0.24 mmol) in DME (20 mL) at -60°C, a solution of sulfur (15.4 mg, 0.48 mmol) in DME (5 mL) was added. The color of the reaction mixture turned from dark olive green to dark red brown at low temperature and then to dark brown-green while slowly warming up to ambient temperature and was stirred for further 18 h at room temperature. The solvent was removed and the product was washed with *n*-hexane, dissolved in THF (10 mL) and the solution was layered with *n*-hexane (30 ml). After 4 days at 0°C dark green needles of $[K_2(THF)_2]$[**3**] were formed (110mg, 69%)..

Synthesis of $[K_2(DME)_2][3]$ from $[K_2(DME)_2][B]$ and sulfur:

To a solution of $[K_2(DME)_2]$[**B**] (100 mg, 0.17 mmol) in DME (20 mL) at -60°C, a solution of sulfur (10.6 mg, 0.33 mmol) in DME (5 mL) was added. The color of the reaction mixture turned from dark olive green to dark brown-green while slowly warming up to ambient temperature and was stirred for further 18 h at room temperature. The crude mixture was layered with with *n*-hexane (20 ml) and left for 4 days at 0°C from which dark green crystalline precipitate of $[K_2(DME)_2]$[**3**] was formed (88mg, 78%).

^{1}H NMR (THF-d_8):	δ [ppm] = 1.63 (s, 15 H, $C_5(CH_3)_5$), 3.28 (s, 12 H, CH_3, DME), 3.44 (s, 8 H, CH_2, DME).
^{13}C{^{1}H} NMR (THF-d_8):	δ [ppm] = 11.7 (s, $C_5(CH_3)_5$), 58.7 (s, CH_3, DME), 72.7 (s, CH_2, DME), 86.0 (s, $C_5(CH_3)_5$).
^{31}P NMR (THF-d_8):	δ [ppm] = -8.7 (m, 2 P), 21.2 (m, 2 P), 182.8 (t, 1 P).
^{31}P{^{1}H} NMR (THF-d_8):	δ [ppm] = -8.7 (m, 2 P), 21.2 (m, 2 P), 182.8 (t, 1 P).
ES-MS (THF):	*m/z*: 314.8 (15) $[Cp^*FeP_4H]^-$, 346.7 (7) $[Cp^*FeP_5H]^-$, 408.8 (100) $[C_{10}H_{14}FeP_5S_2]^-$.
EA:	calculated for $C_{10}H_{15}FeK_2P_5S_2 \bullet 1.3\ C_4H_{10}O_2$: C: 30.16%, H: 4.66%, S: 10.59%; found: C: 30.32%, H: 4.78%, S: 12.31%.

1.5 Synthesis and characterization of $[K_2(THF)_4][4]$, $[4] = [Cp^*Fe(\eta^4\text{-}P_5Se_2)]^{2-}$:

To a solution of $K_2(DME)_3$][**C**] (250 mg, 0.24 mmol) in DME (20 mL) at -60°C, a suspension of selenium (38.0 mg, 0.48 mmol) in DME (10 mL) was added. The color of the reaction mixture turned from dark olive green to dark red at low temperature then to dark brown-green while slowly warming up to ambient temperature and was stirred for further 2 h at room temperature. The solvent was removed and the product was washed with *n*-hexane, dissolved in THF (10 mL) and the solution was layered with *n*-hexane (30 mL). After 2 days at 0 °C brown blocks of $[K_2(THF)_4]$[**4**] were formed (120 mg, 65%).

Synthesis of $[K_2(DME)_2]$[4] from $[K_2(DME)_2]$[B] and selenium:

To a solution of $[K_2(DME)_2]$[**B**] (70 mg, 0.14 mmol) in DME (20 mL) at -60°C, a suspension of selenium (22 mg, 0.28 mmol) in DME (5 mL) was added. The color of the reaction mixture turned from dark olive green to dark brown while slowly warming up to ambient temperature and was stirred for further 30 min at room temperature. The solvent was removed and $[K_2(DME)_2]$[**4**] was obtained as dark brown powder (83 mg, 79%).

^{1}H NMR (THF-d_8):	δ [ppm] = 1.61 (s, 15 H, $C_5(CH_3)_5$), 3.28 (s, 12 H, CH_3, DME), 3.44 (s, 8 H, CH_2, DME).
^{13}C{^{1}H} NMR (THF-d_8):	δ [ppm] = 11.6 (s, $C_5(CH_3)_5$), 58.9 (s, CH_3, DME), 72.7 (s, CH_2, DME), 86.1 (s, $C_5(CH_3)_5$).
^{31}P NMR (THF-d_8):	δ [ppm] = 0.7 (m, 2 P), 23.0 (m, 2 P), 116.6 (t, 1 P).
^{31}P{^{1}H} NMR (THF-d_8):	δ [ppm] = 0.7 (m, 2 P), 23.0 (m, 2 P), 116.6 (t, 1 P).
^{77}Se NMR (THF-d_8):	δ [ppm] = -64.4 (d, $^{1}J_{(Se,P)}$ = 471 Hz, 1 Se), 560.1 (d, $^{1}J_{(Se,P)}$ = 530 Hz, 1 Se).
EA:	calculated for $C_{10}H_{15}FeK_2P_5Se_2$ • 1.3 $C_4H_{10}O_2$: C: 26.11%, H: 4.04%; found: C: 25.73%, H: 4.05%.

1.6 Synthesis and characterization of $[K_2(DME)_2]$[5], [5] = $[Cp^*Fe(\eta^4\text{-}P_5SSe)]^{2-}$:

To a solution of $[K_2(DME)_2]$[**1**] (127 mg, 0.20 mmol; prepared in situ from $[K_2(DME)_2]$[**B**] and sulfur) in DME (20 mL) at room temperature, a suspension of selenium (15.8 mg, 0.20 mmol) in DME (5 mL) was added. The reaction mixture was stirred overnight, then the volume of solvent was reduced to its half in vacuum, the reaction mixture was layered with *n*-hexane (30 mL) and stored at r.t. After 2 days, dark green plates of $[K_2(DME)_2]$[**5**] were formed.

Yield:	100 mg (69%).
^{1}H NMR (THF-d_8):	δ [ppm] = 1.61 (s, 15 H, $C_5(CH_3)_5$), 3.28 (s, 12 H, CH_3, DME), 3.43 (s, 8 H, CH_2, DME).
^{31}P NMR (THF-d_8):	δ [ppm] = 152.1 (s, 2 P), 143.4 (m, 1 P), 23.1 (m, 2 P), −0.5 (m, 2 P).
^{31}P{^{1}H} NMR (THF-d_8):	δ [ppm] = 152.1 (s, 2 P), 143.4 (m, 1 P), 23.1 (m, 2 P), −0.5 (m, 2 P).
^{77}Se NMR (THF-d_8):	δ [ppm] = −83.6 (m, $^{1}J_{Se\text{-}P}$ = 480.6 Hz).
ESI-MS (DME):	*m/z*: 458.92 (55 %, $[MH]^+$), 378.9 (100 %, $[Cp^*Fe(\eta^4\text{-}P_5O_2)^-H]^+$).

$[K_2(DME)_2]$[**5**] can also be prepared by *in situ* preparation of $[K_2(DME)_2]$[**1**] from $[K_2(DME)_2]$[**B**] and sulfur in DME at room temperature first and adding a suspension of selenium in DME. By using the same amounts as above mentioned, the yield is slightly higher (71%).

1.7 Synthesis and characterization of [K][6], [6] = $[Cp^*Fe(\eta^4\text{-}P_5OH)]^-$:

A mixture of KOH (117 mg, 2.10 mmol) and $[Cp^*Fe(\eta^5\text{-}P_5)]$ (800 mg, 2.30 mmol) are dissolved in DME (130 mL) and stirred for three days at room temperature during which a change in the color of the reaction mixture from green to dark brown was observed. The solvent was removed and the precipitate was washed with *n*-hexane, dried in vacuum for 3 hours from which K[**6**] was isolated. Crystals of

[Li(THF)$_2$][**6**] suitable for X-ray structure analysis were obtained from a similar reaction of [Cp*Fe(η^5-P_5)] with LiOH.

Yield:	500 mg (54%).
^{1}H NMR (THF-d_8):	δ [ppm] = 1.50 (s, 15 H, $C_5(CH_3)_5$), 7.5 (dtt, $^1J_{(H,P)}$ = 364,6 Hz, $^2J_{(H,P)}$ = 45.9 Hz, $^2J_{(H,P)}$ = 5.6 Hz; 1 H, P-H).
^{31}P NMR (THF-d_8):	δ [ppm] = -17.55 (m, 1 P), 19.0 (m, 2 P), 80.9 (m, 1 P).
^{13}C{^{1}H} NMR (THF-d_8):	11.6 (s, $C_5(CH_3)_5$), 87.3 (s, $C_5(CH_3)_5$).
EA:	calculated for $C_{10}H_{16}FeP_5OK$: C: 29.87%, H: 4.01%; found: C: 30.14%, H: 3.99%.

1.8 Synthesis and characterization of [K_2(DME)$_2$][7], [7] = [Cp*Fe(η^4-P_5O)]$^{2-}$:

A mixture of K (13 mg, 0.33 mmol) and K[Cp*Fe(η^5-POH)] (80 mg, 0.23 mmol) are dissolved in DME (15 mL) and stirred for three days at room temperature resulting in a dark brown-greenish solution. The solution was filtered, the solvent removed, dried in vacuum for 3 hours from which [K_2(DME)$_2$][**7**] was isolated.

Yield:	59 mg (67%).
^{1}H NMR (THF-d_8):	δ [ppm] = 1.32 (s, 15 H, $C_5(CH_3)_5$)
^{31}P NMR (THF-d_8):	δ [ppm] = 20.9 (m, 2 P), 35.6 (m, 2 P), 165.4 (m, 2 P).
^{13}C{^{1}H} NMR (THF-d_8):	δ [ppm] = 11.6 (s, $C_5(CH_3)_5$), 85.4 (s, $C_5(CH_3)_5$).
EA:	calculated for $C_{10}H_{15}FeP_5K_2$: C: 27.29%, H: 3.44%; found: C: 27.30%, H: 3.70%.

1.9 Synthesis and characterization of [K(18c6)]$_2$[Cp*Fe(η^4-P_5O_2)] (8):

To a solution of [K_2(DME)$_2$][**1**] (127 mg, 0.20 mmol) in DME (20 mL) was added to a suspension of Me_3NO (30 mg, 0.40 mmol) in DME (10 mL) at room temperature. In addition, a cold solution of 18c6 (106 mg, 0.40 mmol) in DME (10 mL) was added to the reaction mixture and was stirred overnight. The volume was reduced *in vacuo*, the reaction mixture was layered with toluene and stored at −30 °C. Complex **8** can be obtained as dark green blocks within few days.

Yield:	25 mg (14%).
^{1}H NMR (THF-d_8):	δ [ppm] = 1.65 (s, 15 H, $C_5(CH_3)_5$), 2.73 (s, br, unidentified sideproduct), 3.66 (s, 53 H, 18c6).
^{31}P NMR (THF-d_8):	δ [ppm] = 144.8 (m, 1 P), 2.4 (m, 2 P), −64.8 (m, 2 P).
^{31}P {^{1}H} NMR (THF-d_8):	δ [ppm] = 144.8 (m, 1 P), 2.4 (m, 2 P), −64.8 (m, 2 P).
EA:	No satisfying elemental analysis could be obtained after several attempts of the isolated crystals.

1.10 Synthesis and characterization of [{Na(15c5)thf$_{0.9}$}{Na(15c5)}][Cp*Fe(η^4-P$_5$Te$_2$)] (9):

A mixture of [Cp*Fe(η^5-P$_5$)] (**A**) (104 mg, 0.30 mmol) and Na_2Te (51 mg, 0.30 mmol) were dissolved in DME (15 mL). To the resulting suspension, a 0.67 molar solution of 15c5 in DME (0.80 mmol, 1.2 mL) was added. The mixture was stirred overnight. Thereby, the color changed to red/brown and a colorless solid is formed. The volume was reduced *in vacuo* and filtered over a glass frit. The solvent was removed under reduced pressure, the residue dissolved in THF, layered with *n*-hexane and stored at room temperature. Complex [{Na(15c5)thf$_{0.9}$}{Na(15c5)}][**9**] was obtained as dark green plates.

Yield:	78 mg (22%).
^{1}H NMR (THF-d$_8$):	δ [ppm] = 1.52 (s, 12 H, unidentified side product), 1.58 (s, 15 H, C$_5$(C*H*$_3$)$_5$), 1.77 (m, 8 H, THF), 3.61 (m, 8 H, THF), 3.66 (s, 53 H, 18c6). 3.75 (s, 68 H, 15c5).
^{31}P NMR (THF-d$_8$):	δ [ppm] = 80.9 (m, 1 P), 26.6 (m, 3 P), 4.5 (m, 2 P).
^{31}P {^{1}H} NMR (THF-d$_8$):	δ [ppm] = 80.9 (m, 1 P), 26.6 (m, 3 P), 4.5 (m, 2 P).
ESI-MS (DME):	*m/z*: 362.96 (100 %, [Cp*Fe(η^4-P$_5$OH)]$^+$).

1.11 Synthesis and characterization of [{Na(15c5)}{Na(Ph$_3$PO)(15c5)}][Cp*Fe(η^4-P$_5$Te$_2$)] (9´):

To a solution of complex **9** (100.0 mg, 0.09 mmol) in THF (15 mL) Ph_3PO (30.9 mg 0.11 mmol) was added in THF (15 mL) and the reaction mixture was stirred for 30 minutes. No color change was observed, but grey tellurium was formed. The solvent was removed under reduced pressure. The residue was washed with toluene, extracted with THF and filtered over diatomaceous earth. The volume of the filtrate was reduced, layered with *n*-hexane and stored at room temperature. Complex **9´** was obtained as dark green blocks.

Yield:	90 mg (73%).
^{1}H NMR (THF-d$_8$):	7.56 (m, 15 H, Ph$_3$PO), 3.75 (s, 92 H, 15c5), 3.61 (m, 4 H, THF), 1.77 (m, 4 H, THF), 1.58 (m, 25 H, unidentified side product), 1.53 (m, 15 H, C$_5$(C*H*$_3$)$_5$).
^{31}P NMR (THF-d$_8$):	δ [ppm] = 81.0 (m, 1 P), 26.2 (m, 2 P), 24.9 (s, 1 P, Ph$_3$PO), 5.0 (m, 2 P).
^{31}P {^{1}H} NMR (THF-d$_8$):	δ [ppm] = 81.0 (m, 1 P), 26.2 (m, 2 P), 24.9 (s, 1 P, Ph$_3$PO), 5.0 (m, 2 P).

2. NMR Spectra:

The ^{31}P NMR spectra of **1**-**4** are of high order. To determine the coupling constants of the P atoms, the ^{31}P NMR spectrum of each anion was simulated with the software TOPSPIN 3.0.

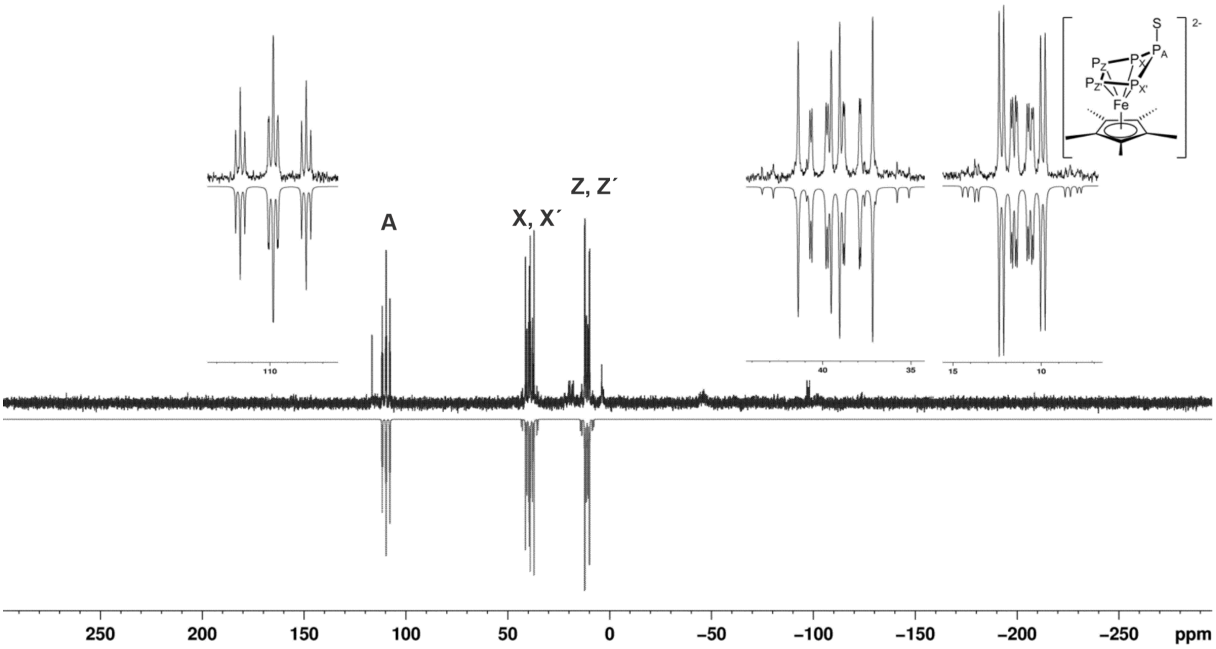

Fig. S1 Experimental (top) and simulated (bottom) ^{31}P NMR (161.97 MHz, DME/DMSO-d_6) spectrum of $[K_2(DME)_2]$[**1**].

Table S1. ^{31}P NMR chemical shifts and coupling constants for $[K_2(DME)_2]$[**1**] obtained from the simulation of the ^{31}P NMR (161.97 MHz, DME/DMSO-d_6) spectrum.

J (Hz)		δ (ppm)	
$^1J_{PA-PX} = {}^1J_{PA-PX'}$	303.36	$P_{Z,Z'}$	11.1
$^2J_{PA-PZ} = {}^2J_{PA-PZ'}$	-42.62	$P_{X,X'}$	39.2
$^2J_{PX-PX'}$	-60.51	P_A	109.8
$^2J_{PX-PZ'} = {}^2J_{PX'-PZ'}$	375.56		
$^2J_{PX-PZ'} = {}^2J_{PX'-PZ}$	4.35		
$^1J_{PZ'-PZ}$	396.55		

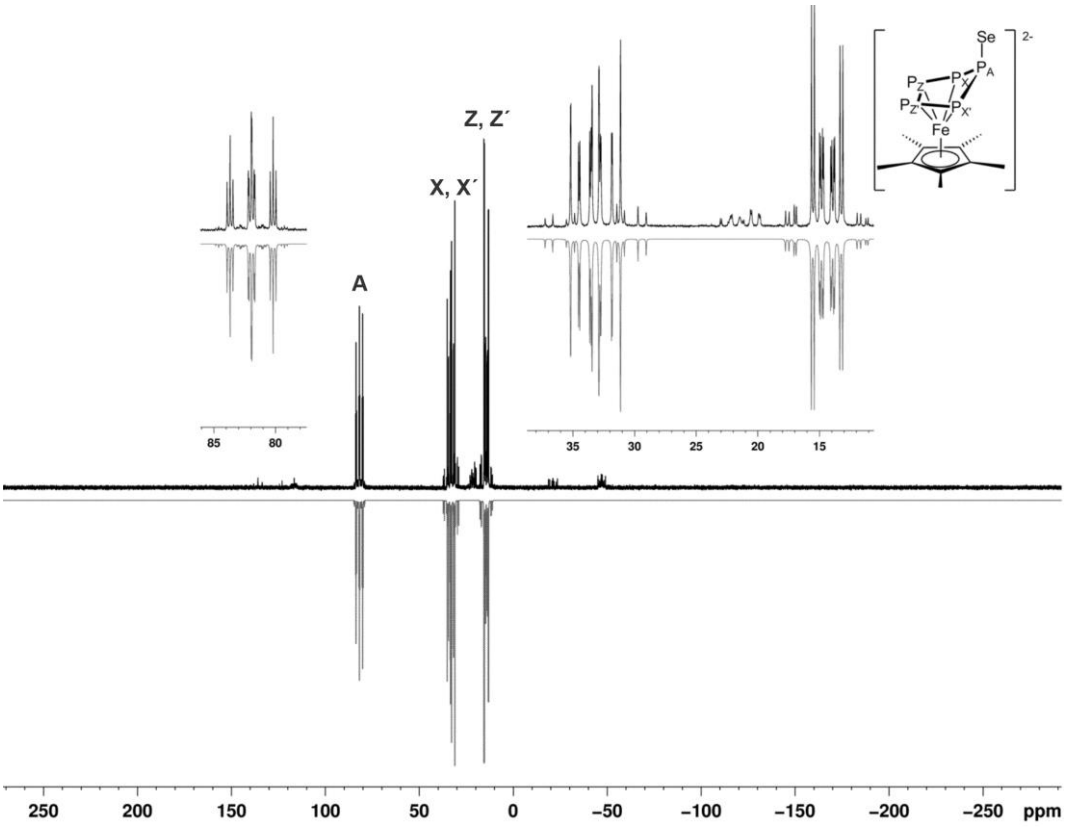

Fig. S2 Experimental (top) and simulated (bottom) ^{31}P NMR (161.97 MHz, THF-d_8) spectrum of [K_2(DME)$_2$][**2**].

Table S2. ^{31}P NMR chemical shifts and coupling constants for [K_2(DME)$_2$][**2**] obtained from the simulation of the ^{31}P NMR (161.97 MHz, THF-d_8) spectrum.

J (Hz)				δ (ppm)	
$^1J_{PA-PX}$	284.21	$^1J_{PX-PZ}$	371.41	$P_{Z,Z'}$	14.5
$^1J_{PA-PX'}$	284.23	$^2J_{PX-PZ'}$	1.27	$P_{X,X'}$	33.1
$^2J_{PA-PZ}$	-39.79	$^2J_{PX'-PZ}$	1.19	P_A	81.9
$^2J_{PA-PZ'}$	-39.78	$^1J_{PX'-PZ'}$	371.46		
$^2J_{PX-PX'}$	-59.25	$^1J_{PZ'-PZ}$	399.46		
$^1J_{PA-Se}$	300.02				

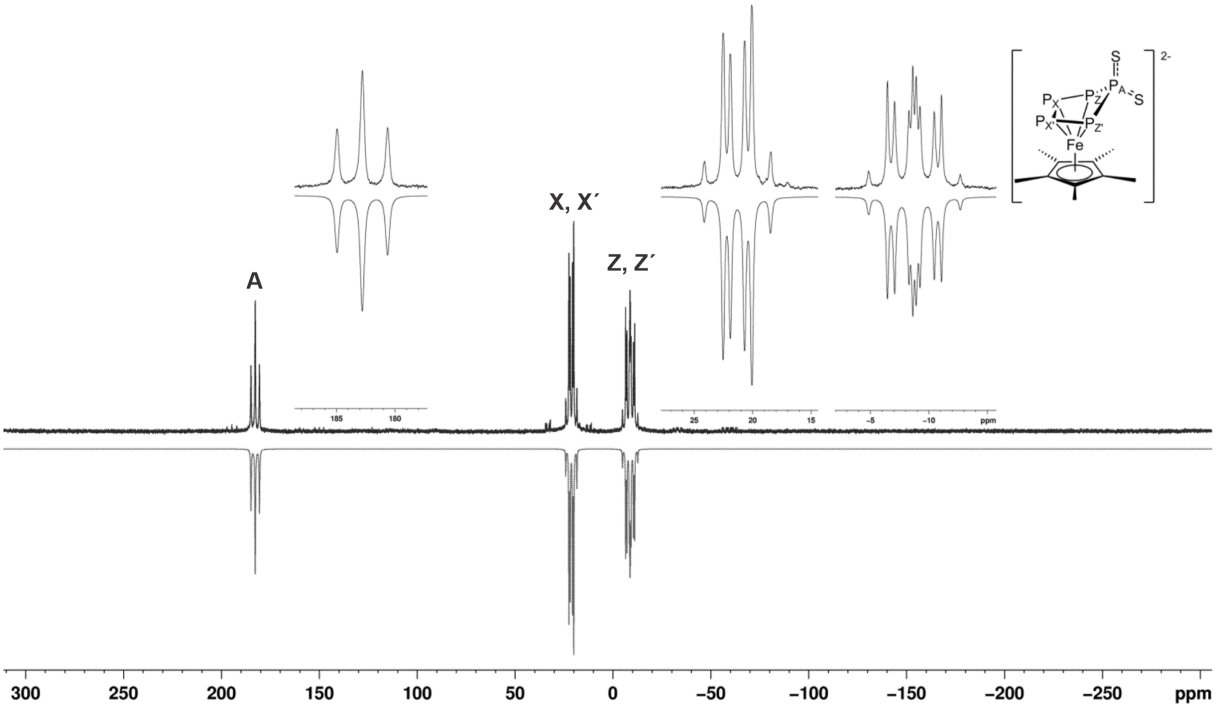

Fig. S3 Experimental (top) and simulated (bottom) ^{31}P NMR (161.97 MHz, THF-d_8) spectrum of $[K_2(DME)_2]$[**3**].

Table S3. ^{31}P NMR chemical shifts and coupling constants for $[K_2(DME)_2]$[**3**] obtained from the simulation of the ^{31}P NMR (161.97 MHz, THF-d_8) spectrum.

J (Hz)		δ (ppm)	
$^1J_{PA-PX} = {}^1J_{PA-PX'}$	-17.16	$P_{Z,Z'}$	-8.7
$^2J_{PA-PZ} = {}^2J_{PA-PZ'}$	351.11	$P_{X,X'}$	21.2
$^2J_{PX-PX'}$	362.62	P_A	182.8
$^1J_{PX-PZ} = {}^1J_{PX'-PZ'}$	411.16		
$^2J_{PX-PZ'} = {}^2J_{PX'-PZ}$	-13.39		
$^2J_{PZ'-PZ}$	9.28		

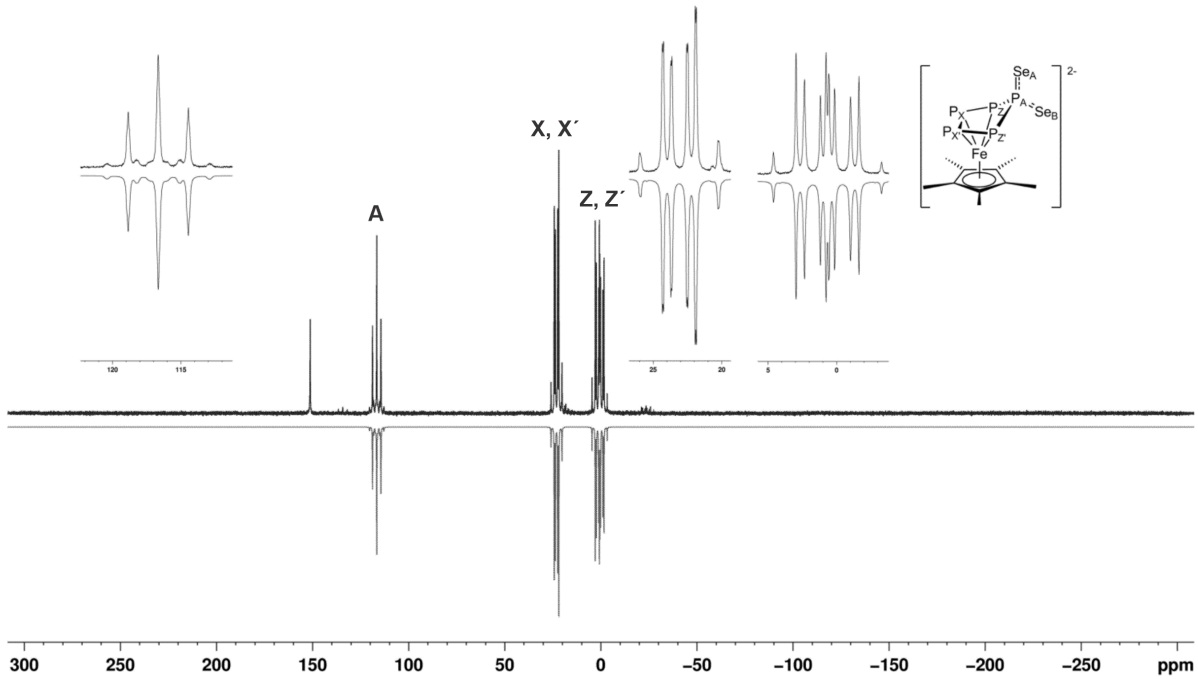

Fig. S4 Experimental (top) and simulated (bottom) ^{31}P NMR (161.97 MHz, THF-d_8) spectrum of [K_2(DME)$_2$][**4**].

Table S4. ^{31}P NMR chemical shifts and coupling constants for [K_2(DME)$_2$][**4**] obtained from the simulation of the ^{31}P NMR (161.97 MHz, THF-d_8) spectrum.

J (Hz)				δ (ppm)	
$^2J_{PA-PX}$	-16.89	$^1J_{PX-PZ}$	401.67	$P_{Z,Z'}$	0.7
$^2J_{PA-PX'}$	-16.92	$^2J_{PX-PZ'}$	-14.61	$P_{X,X'}$	23.0
$^1J_{PA-PZ}$	355.87	$^2J_{PX'-PZ}$	-14.49	P_A	116.6
$^1J_{PA-PZ'}$	355.86	$^1J_{PX'-PZ'}$	401.76		
$^1J_{PX-PX'}$	369.74	$^2J_{PZ'-PZ}$	0.91		
$^1J_{PA-SeA}$	530.15	$^1J_{PA-SeB}$	471.14		

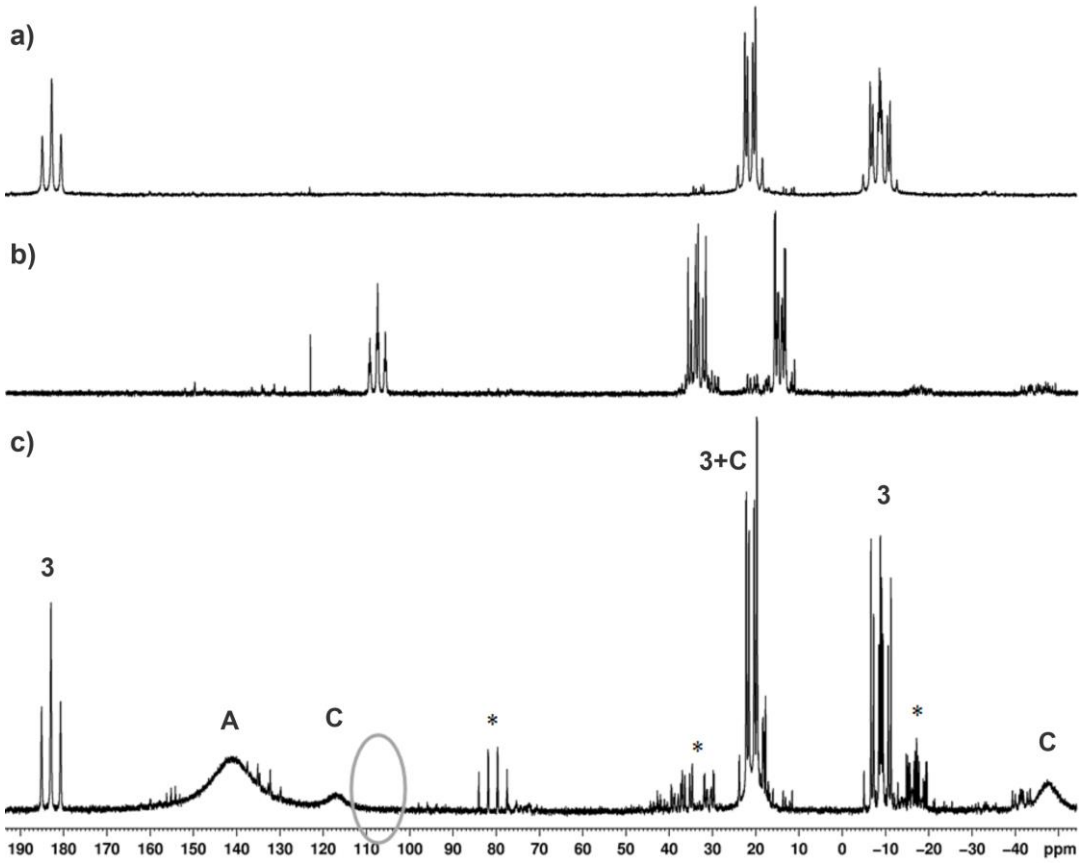

Fig. S5 Experimental ^{31}P NMR (161.97 MHz, THF-d_8) spectrum of: a) $[K_2(DME)_2]$[**3**], b) $[K_2(DME)_2]$[**1**] and c) the reaction of $[K_2(DME)_3]$[**C**] with one equivalent of sulfur. In c) the signals are assigned to the corresponding anions. The characteristic signals of **1** are missing (region marked with grey circle). Impurities are marked with*.

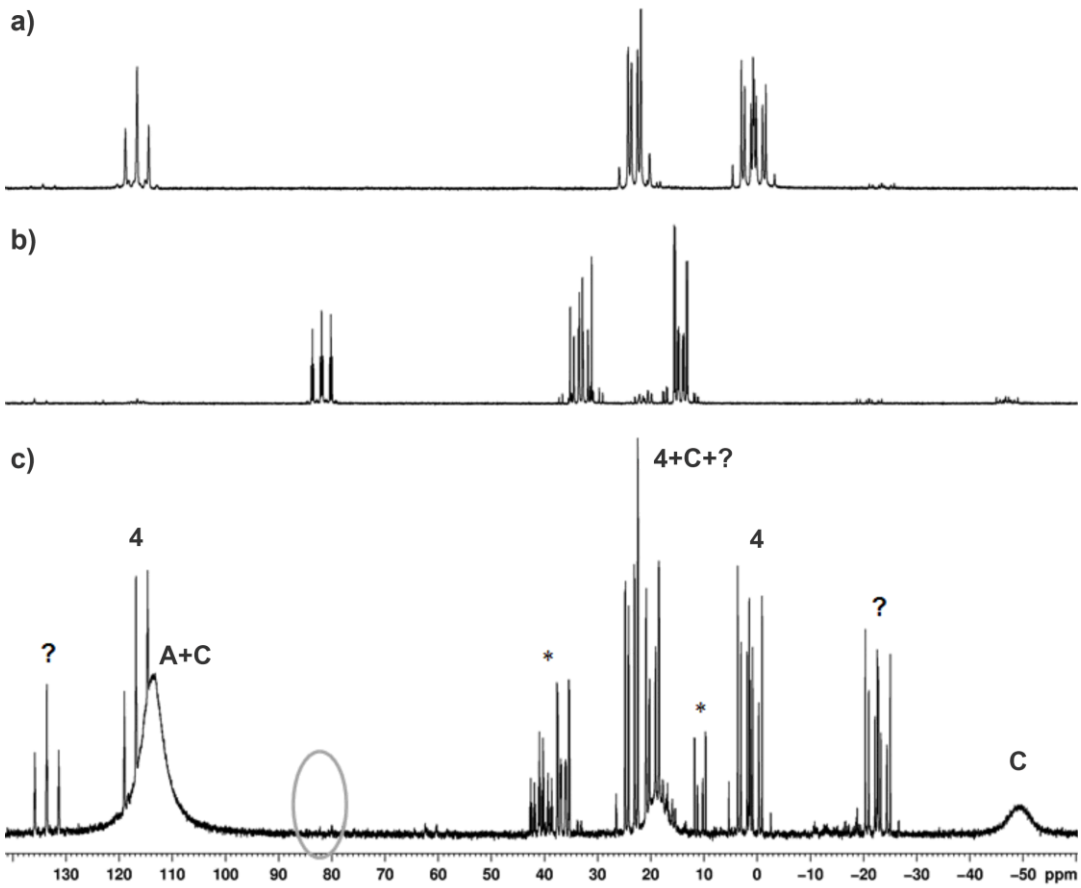

Fig. S6 Experimental ^{31}P NMR (161.97 MHz, THF-d_8) spectrum of: a) [K_2(DME)$_2$][**4**], b) [K_2(DME)$_2$][**2**] and c) the reaction of [K_2(DME)$_3$][**C**] with one equivalent of selenium. In c) the signals are assigned to the corresponding anions. The characteristic signals of **2** are missing (region marked with grey circle). A non-identified byproduct is marked with '?'. Impurities are marked with*.

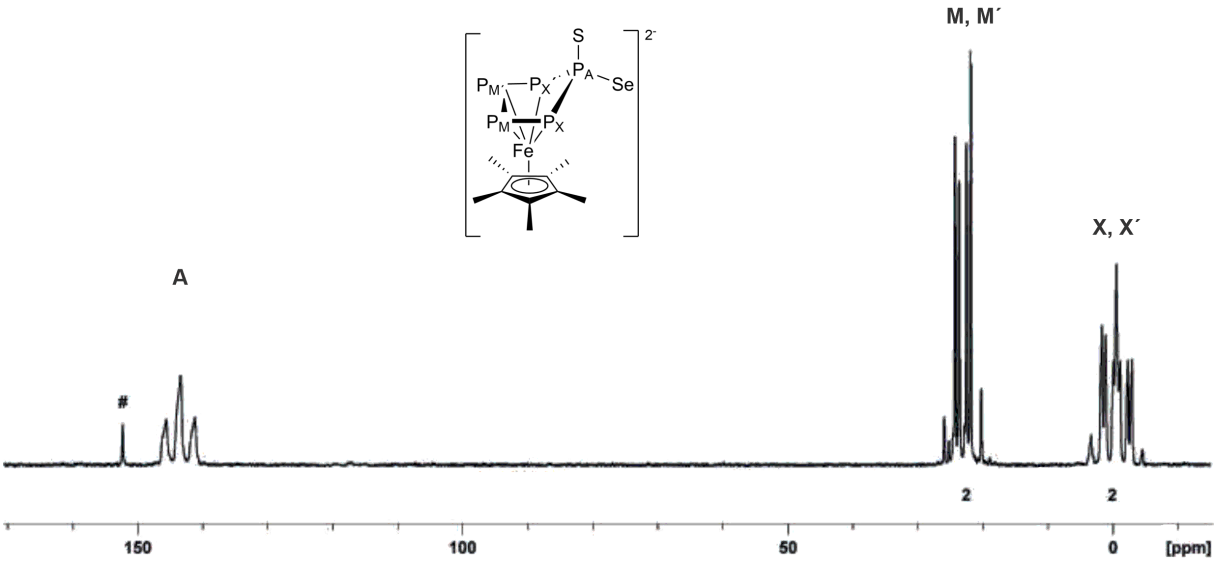

Fig. S7 $^{31}P\{^{1}H\}$ NMR (161.97 MHz, THF-d_8) spectrum of $[K_2(DME)_2]$[**5**]. # = Compound **A**.

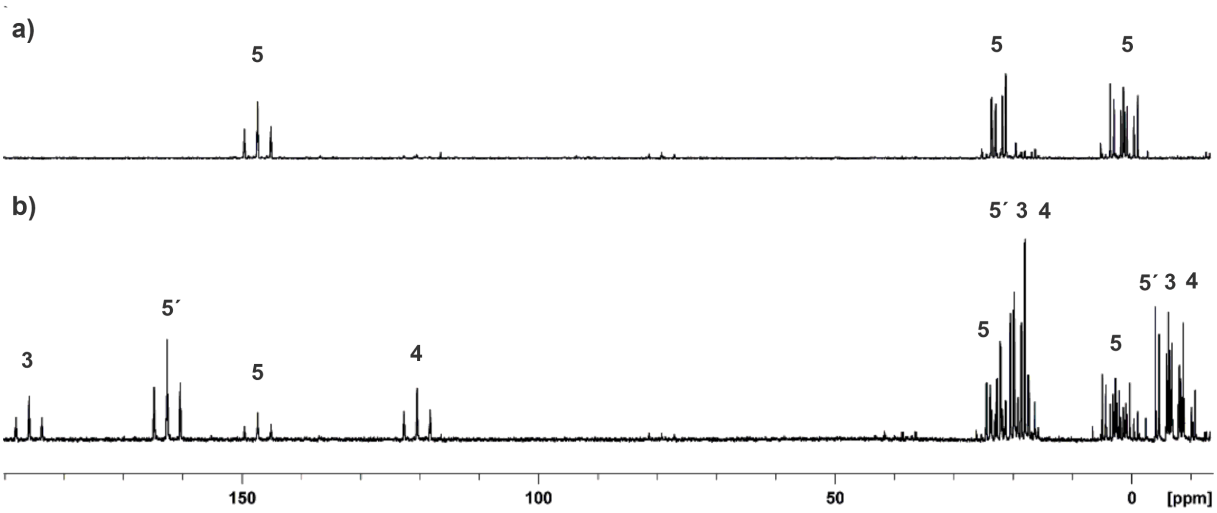

Fig. S8 $^{31}P\{^{1}H\}$ NMR spectra (161.97 MHz, DME/C_6D_6 capillary); a) the reaction of $[K_2(DME)_2]$[**B**] with one equivalent of sulfur then selenium. b) the reaction of $[K_2(DME)_2]$[**B**] with one equivalent of selenium then sulfur. The signals are assigned to the corresponding compound number. Compound **5´** = $[K(DME)_2]_2[Cp^*Fe(\eta^4\text{-}P_5SeS)]$.

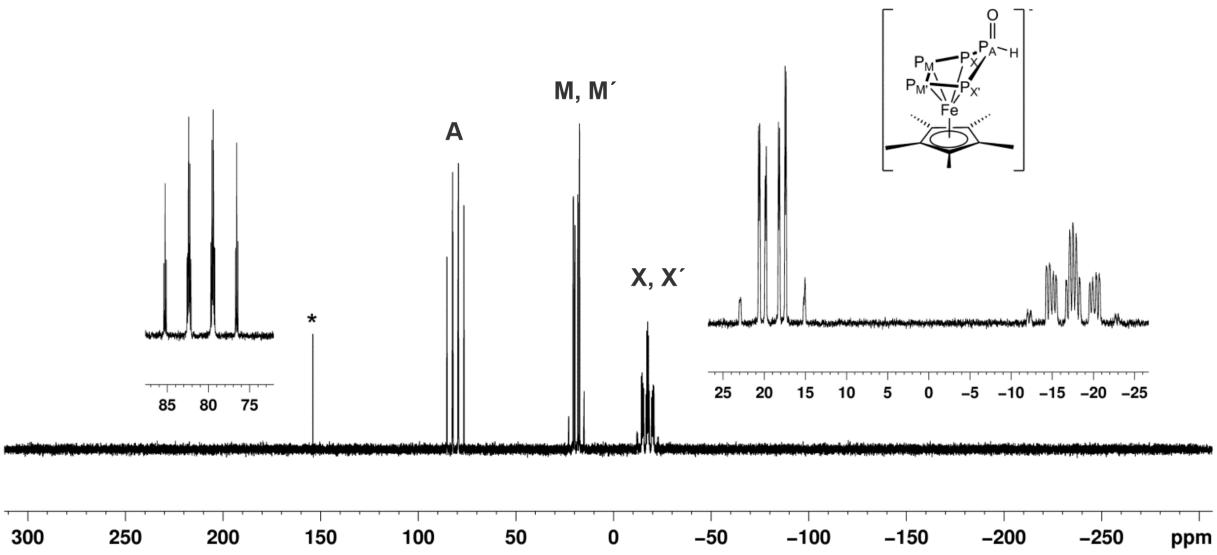

Fig. S9 ^{31}P NMR (161.97 MHz, THF-d_8) spectrum of [$Li_2(THF)_2$][**6**]. Impurities of compound **A** are marked with *.

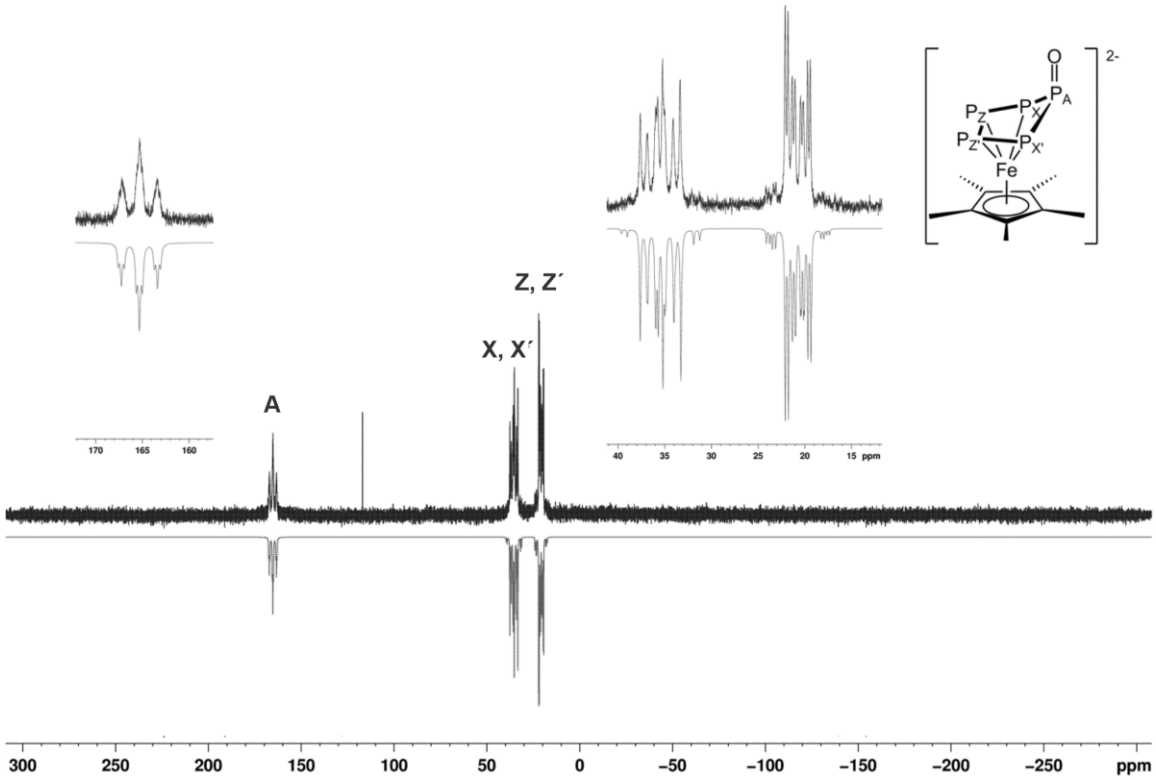

Fig. S10 Experimental (top) and simulated (bottom) ^{31}P NMR (161.97 MHz, THF-d_8) spectrum of [$K_2(DME)_2$][**7**]•0.5 C_7H_8.

Table S5. Spectral parameters for an AXX'ZZ' spin system obtained from the simulation of the ^{31}P NMR (161.97 MHz, THF-d_8) spectrum of [K_2(DME)$_2$][**7**].

J (Hz)		δ (ppm)	
$^1J_{PA-PX} = {}^1J_{PA-PX'}$	315.37	$P_{Z,Z'}$	20.9
$^2J_{PA-PZ} = {}^2J_{PA-PZ'}$	-56.65	$P_{X,X'}$	35.4
$^1J_{PX-PZ} = {}^1J_{PX'-PZ'}$	379.52	P_A	165.3
$^2J_{PX-PZ'} = {}^2J_{PX'-PZ}$	15.32		
$^1J_{P'-PZ'}$	59.25		

3. Crystallographic Data:

The crystal structure analyses were performed on an Agilent Technologies (former Oxford Diffraction) Gemini R Ultra diffractometer with Cu-Kα radiation ([$K_2(THF)_2$][**3**], [$K_2(THF)_4$][**4**], [{Na(15c5)}{$Na(Ph_3PO)$(15c5)}][**9'**]) and Mo-Kα radiation ([{$Na(15c5)THF_{0.9}$}{Na(15c5)}][**9**]) or on an Agilent SuperNova diffractometer with Cu-Kα radiation ([$Li(THF)_2$][**6**], [$K_2(DME)_2$][**7**]) or on an Agilent Technologies (former Oxford Diffraction) GV1000 diffractometer with Cu-Kα radiation ([$K_2(DME)_2$][**1**], [$K_2(DME)_2$][**2**], [$K_2(DME)_2$][**5**]) and Cu-Kß ([$K(18c6)]_2$[**8**]). The measurements were carried out at 123 K. CrysAlisPro was used for data reduction and an analytical absorption correction was carried out for all compounds.[3] The structures were solved by SHELXT (**1**-**6**, **8**-**9'**) and SHELXS (**7**) employing direct methods and refined with the programs SHELXL 2019/2[4] (**6**), SHELXL 2018/3[4,5] (**9**,**9'**) and olex2.refine[6] (**1**-**5**, **7**,**8**) using anisotropic displacement parameters for all non-hydrogen atoms. Hydrogen atoms were located in idealized positions and refined isotopically according to the riding model. For compounds **1**, **2** and **4** non-spherical form factors in NoSpherA2 were applied.[7] For compound **2**, P2, P3 & P4 were refined anharmonically to 3rd order. The figures of the molecular structures were prepared with the OLEX2 software.[8]

CCDC reference numbers: CCDC-2479896 ([$K_2(DME)_2$][**1**]), CCDC-2479897 ([$K_2(DME)_2$][**2**]), CCDC-2479898 ([$K_2(THF)_2$][**3**]), CCDC-2479899 ([$K_2(THF)_4$][**4**]), CCDC-2479900 ([$K_2(DME)_2$][**5**]), CCDC-2479901 ([$Li(THF)_2$][**6**]), CCDC-2479902 ([$K_2(DME)_2$][**7**]), CCDC-2479903 ([$K(18c6)]_2$[**8**]), CCDC-2479904 ([{$Na(15c5)THF_{0.9}$}{Na(15c5)}][**9**]) and CCDC-2479905 ([{Na(15c5)}{$Na(Ph_3PO)$(15c5)}][**9'**]) contain the supplementary crystallographic data for this paper. These data can be obtained free of charge at www.ccdc.cam.ac.uk/conts/retrieving.html (or from the Cambridge Crystallographic Data Centre, 12 Union Road, Cambridge CB2 1EZ, UK; Fax: + 44-1223-336-033; email: deposit@ccdc.cam.ac.uk).

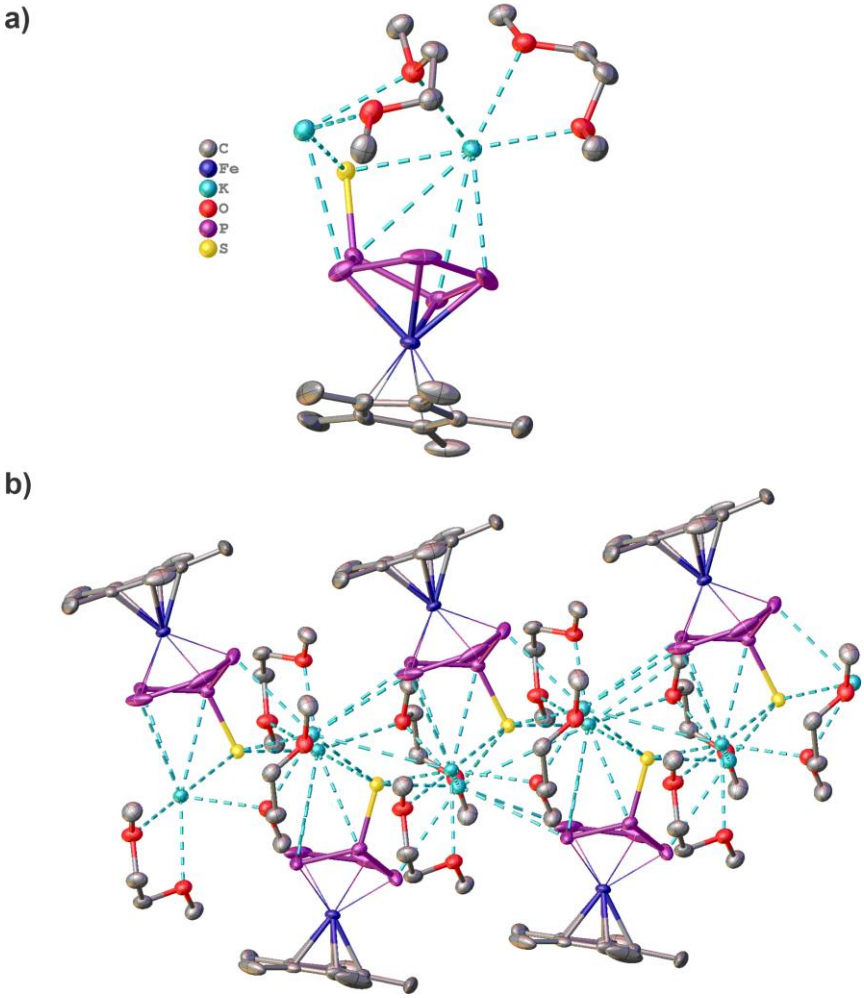

Fig. S11 a) Molecular structure of $[K_2(DME)_2][\mathbf{1}]$ in the solid state. Thermal ellipsoids are drawn with 50% probability. b) Section of the polymeric chain of $[K_2(DME)_2][\mathbf{1}]$. H atoms have been omitted for clarity.

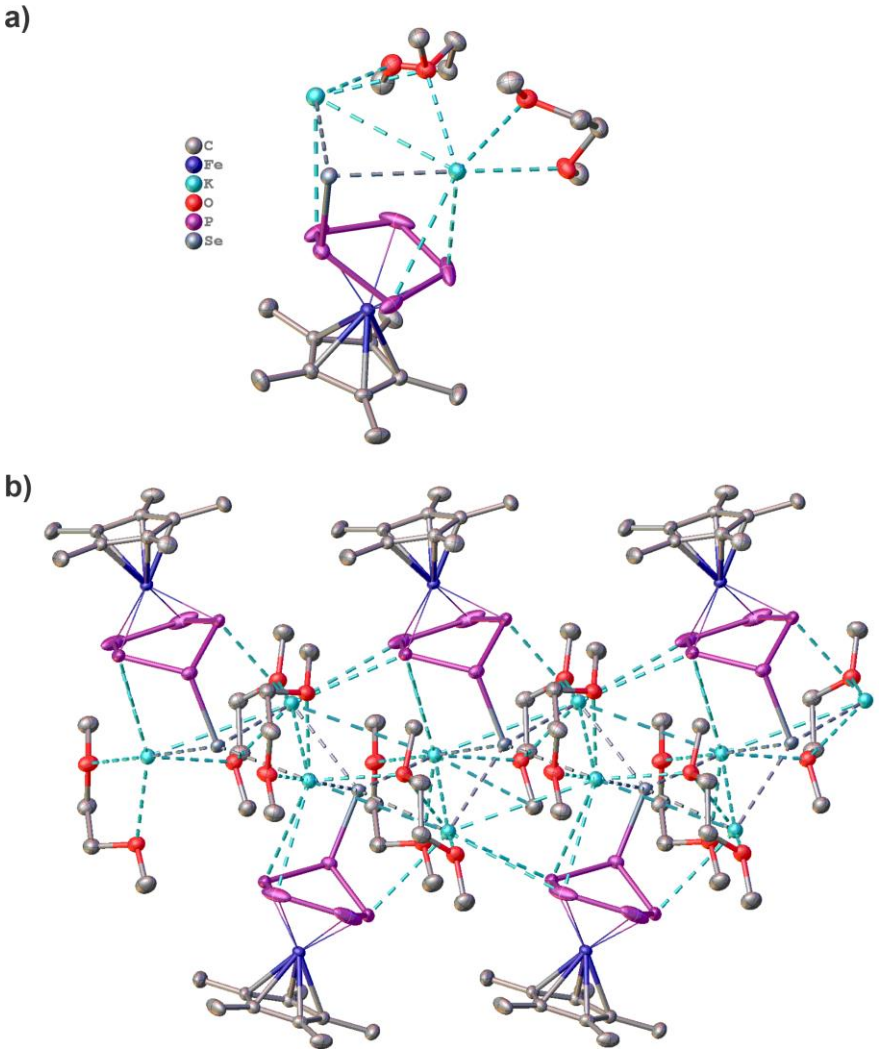

Fig. S12 a) Molecular structure of $[K_2(DME)_2]$[**2**] in the solid state. Thermal ellipsoids are drawn with 50% probability. b) Section of the polymeric chain of $[K_2(DME)_2]$[**2**]. H atoms have been omitted for clarity.

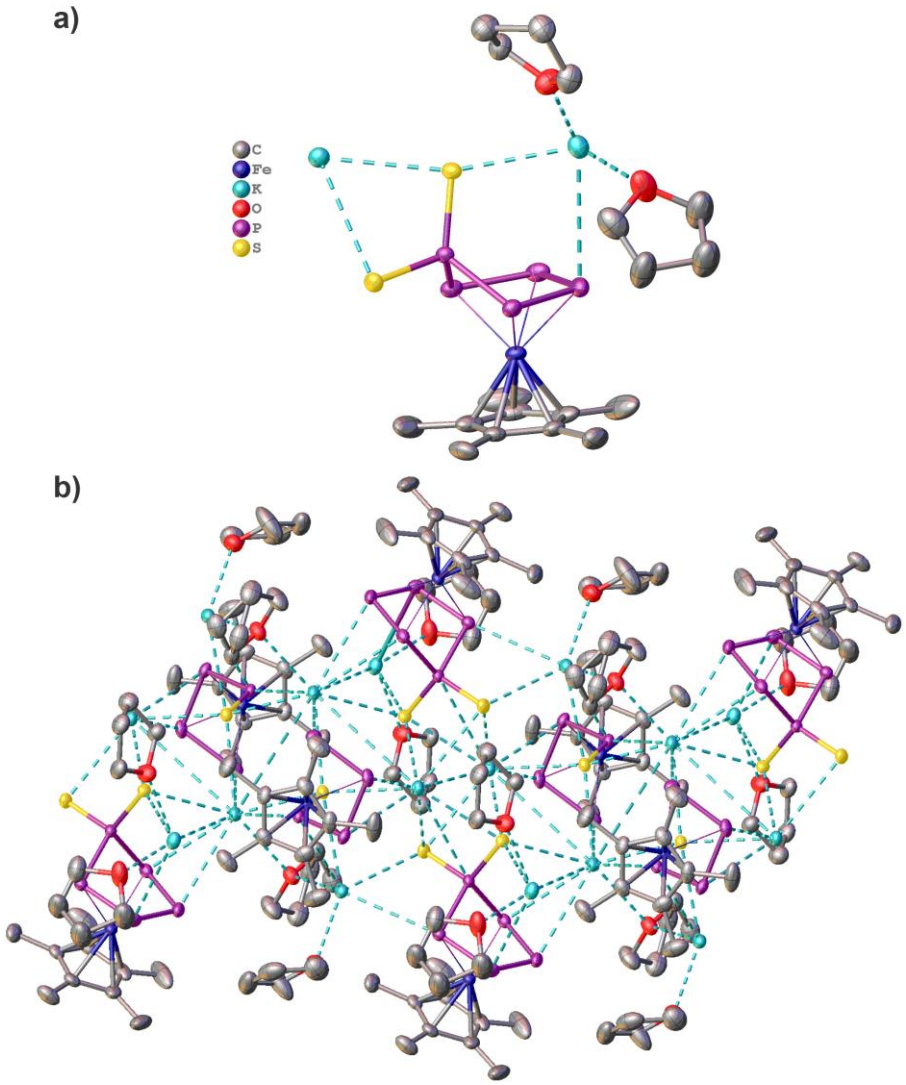

Fig. S13 a) Molecular structure of $[K_2(THF)_2]$[**3**] in the solid state. Thermal ellipsoids are drawn with 50% probability. b) Section of the polymeric chain of $[K_2(THF)_2]$[**3**]. H atoms have been omitted for clarity.

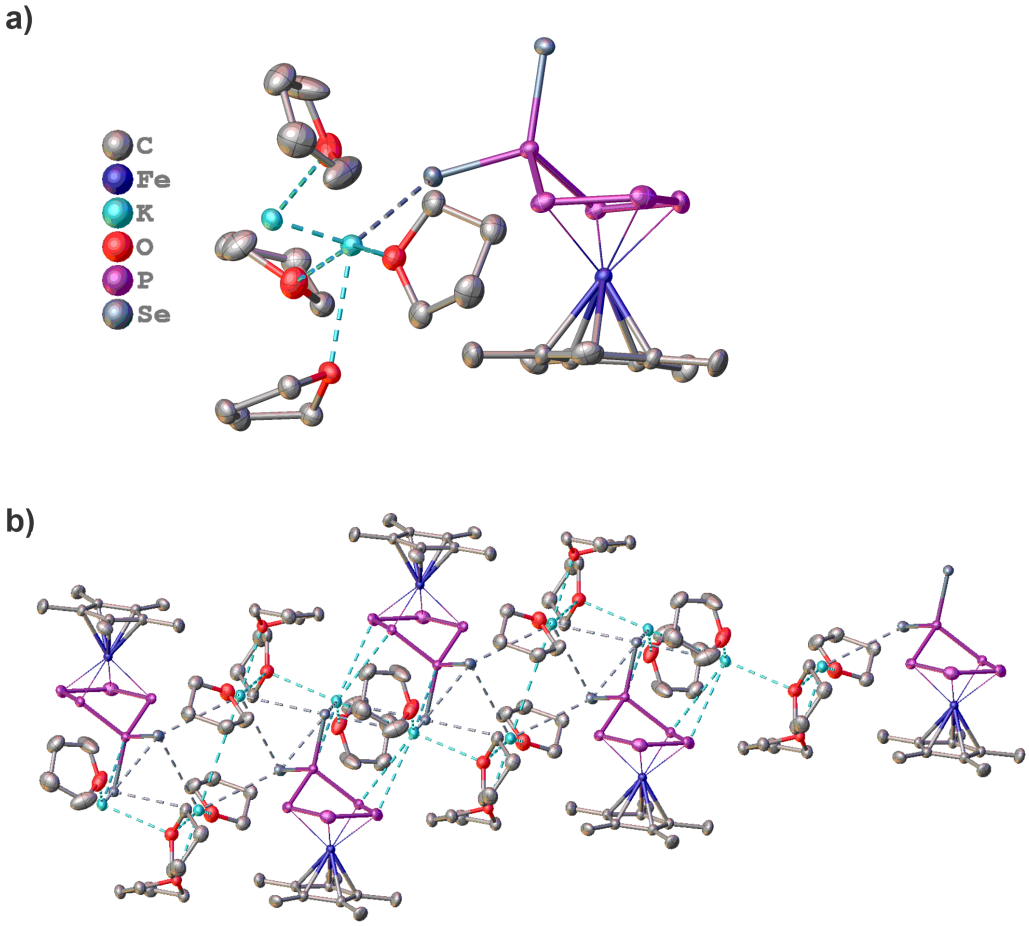

Fig. S14 a) Molecular structure of $[K_2(THF)_4][\mathbf{4}]$ in the solid state. Thermal ellipsoids are drawn with 50% probability. b) Section of the polymeric chain of $[K_2(THF)_4][\mathbf{4}]$. H atoms have been omitted for clarity.

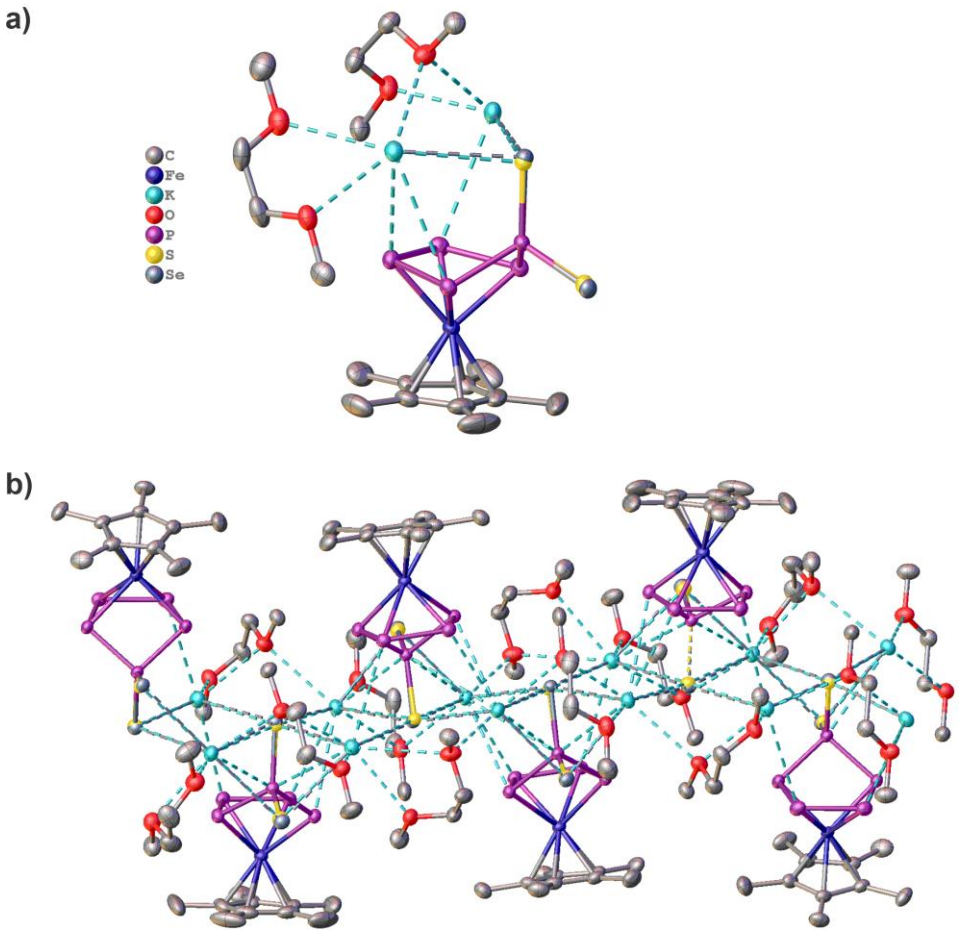

Fig. S15 a) Molecular structure of $[K_2(DME)_2]$[**5**] in the solid state. Thermal ellipsoids are drawn with 50% probability. b) Section of the polymeric chain of $[K_2(DME)_2]$[**5**]. H atoms have been omitted for clarity.

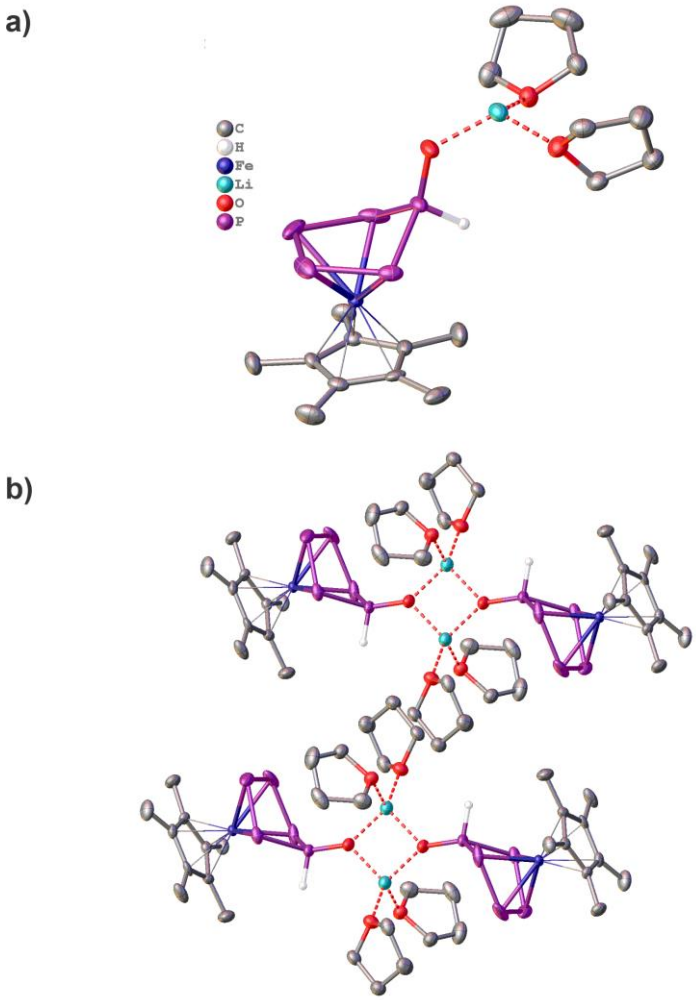

Fig. S16 a) Molecular structure of [Li(THF)$_2$][**6**] in the solid state. Thermal ellipsoids are drawn with 50% probability. b) dimers of [Li(THF)$_2$][**6**] formed bridged by two Li cations. H atoms on C atoms have been omitted for clarity.

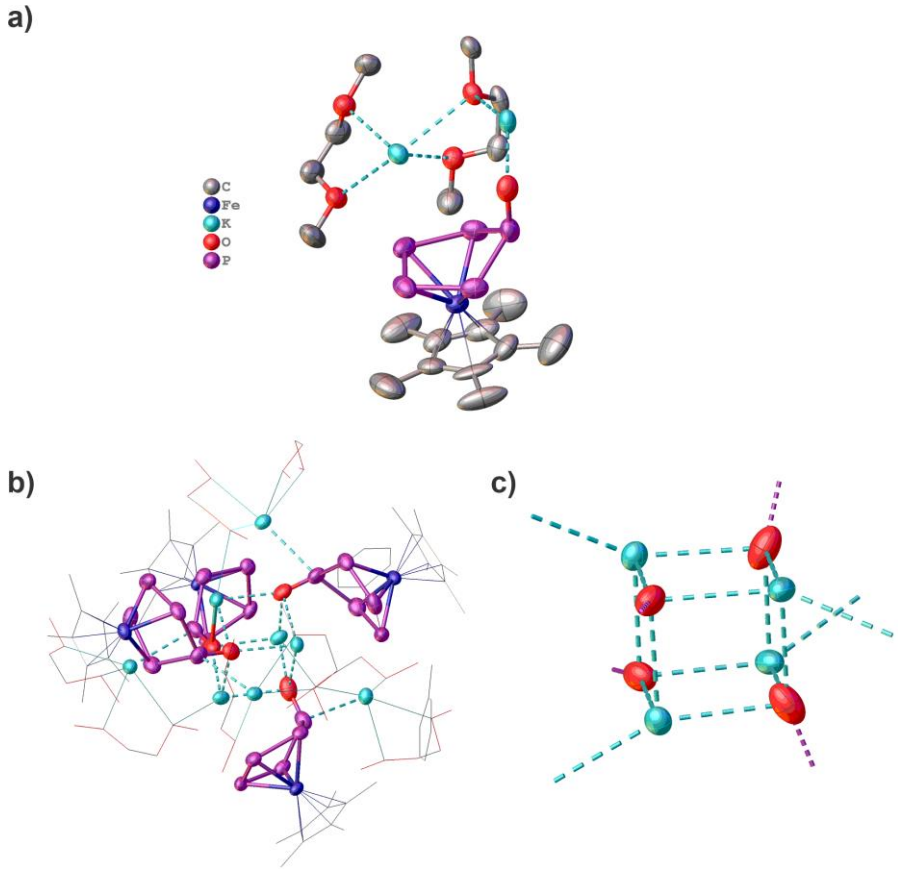

Fig. S17 a) Molecular structure of $[K_2(DME)_2][\mathbf{7}]$ in the solid state. Thermal ellipsoids are drawn with 50% probability. b) tetramer of $[K_8(DME)_8][\mathbf{7}]_4 \bullet 2PhCH_3$ formed bridged by eight K cations and c) view of its K_4O_4 core. H atoms have been omitted for clarity.

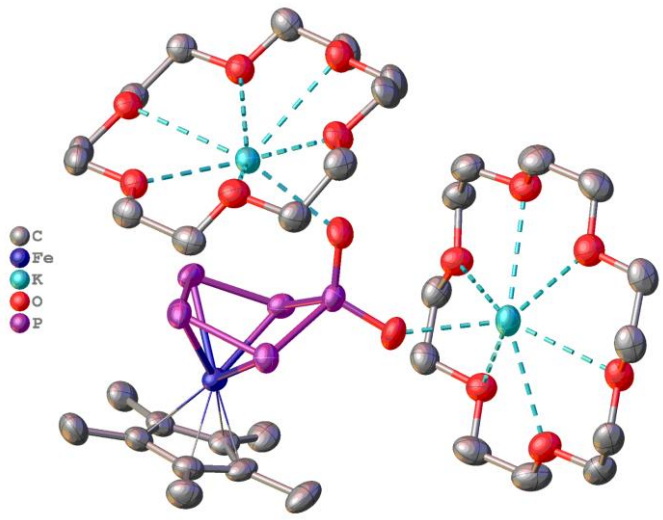

Fig. S18 a) Molecular structure of $[K(18c6)]_2[\mathbf{8}]$ in the solid state. Thermal ellipsoids are drawn with 50% probability. H atoms have been omitted for clarity.

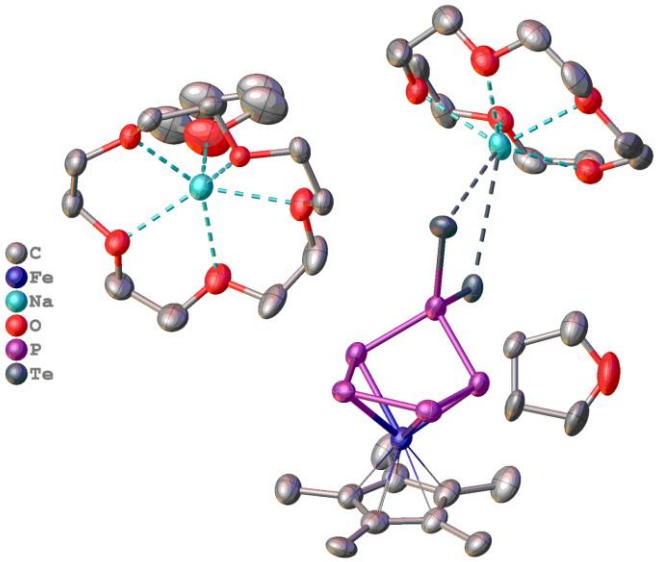

Fig. S19 a) Molecular structure of [{Na(15c5)$THF_{0.9}$}{Na(15c5)}][**9**] in the solid state. Thermal ellipsoids are drawn with 50% probability. H atoms have been omitted for clarity.

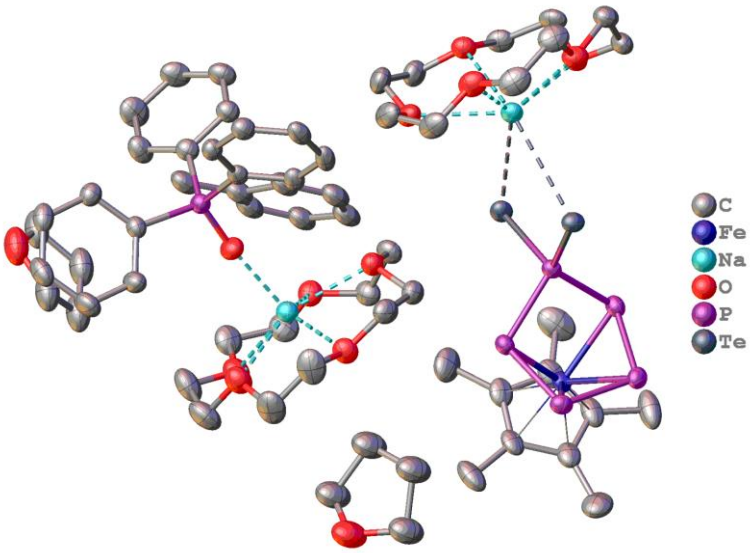

Fig. S20 a) Molecular structure of [{Na(15c5)}{Na(Ph_3PO)(15c5)}][**9'**] in the solid state. Thermal ellipsoids are drawn with 50% probability. H atoms have been omitted for clarity.

Table S6. Crystallographic data for compounds **1**-**3**.

Compound	**1**	**2**	**3**
CCDC-number	2479896	2479897	2479898
Formula	$C_{18}H_{35}FeK_2O_4P_5S$	$C_{18}H_{35}FeK_2O_4P_5Se$	$C_{36}H_{62}Fe_2K_4O_4P_{10}S_4$
Formula Weight	636.453	683.346	1264.977
Temperature/K	122.97(13)	123	126(6)
Crystal System	orthorhombic	monoclinic	triclinic
Space Group	*Pna2₁*	$P2_1/c$	$P\bar{1}$
a/Å	25.9380(4)	13.97112(7)	11.6217(3)
b/Å	13.81698(17)	8.23327(4)	15.4648(4)
c/Å	8.24649(11)	25.98608(13)	18.2721(5)
α/°	90	90	67.695(2)
β/°	90	95.6651(5)	79.084(2
γ/°	90	90	69.783(2)
Volume/Å^3	2955.42(7)	2974.53(3)	2844.69(15)
Z	4	4	2
$D_{calc.}$ / g · cm^{-3}	1.430	1.526	1.477
μ/mm^{-1}	10.027	10.705	11.029
F(000)	1329.6	1397.1	1314.5
Size/mm^3	0.338×0.165×0.09	0.338×0.165×0.09	0.344 × 0.128 × 0.073
Radiation type	CuK_α	CuK_α	CuK_α
Wavelength/Å	1.54184	1.54184	1.54184
2Θ range for data collection/°	6.82 to 148.68	9.8 to 133.64	8.12 to 133.48
Index ranges	-32 ≤ h ≤ 28, -17 ≤ k ≤ 16, -10 ≤ l ≤ 10	-16 ≤ h ≤ 16, -9 ≤ k ≤ 9, -30 ≤ l ≤ 30	-13 ≤ h ≤ 13, -18 ≤ k ≤ 17, -21 ≤ l ≤ 21
Refl. collected	25196	71326	48722
Independent Refl.	5770	5277	10009
R_{int}	0.0955	0.0318	0.0451
R_{sigma}	0.0600	0.0134	0.0308
Data/restraints/ parameters	5770/88/357	5277/0/625	10009/66/593
Goodness-of-fit on F^2	1.031	1.098	1.038
wR_2 (all data)	0.1081	0.0286	0.0745
wR_2	0.1039	0.0283	0.0725
R_1 (all data)	0.0501	0.0129	0.0328
R_1	0.0443	0.0122	0.0295
Largest Peak	0.43	0.19	0.62
Deepest Hole	-0.43	-0.13	-0.32

Table S7. Crystallographic data for compounds **4**-**6**.

Compound	**4**	**5**	**6**
CCDC-number	2479899	2479900	2479901
Formula	$C_{26}H_{47}FeK_2O_4P_5Se_2$	$C_{54}H_{105}Fe_3K_6O_{12}P_{15}S_3Se_3$	$C_{36}H_{64}Li_2O_6P_{10}Fe_2$
Formula Weight	870.490	2146.237	1028.15
Temperature/K	123	123	123(2)
Crystal System	triclinic	triclinic	monoclinic
Space Group	$P\bar{1}$	$P\bar{1}$	$P2_1/c$
a/Å	11.9313(6)	15.0304(2)	15.0254(2)
b/Å	12.4517(4)	18.4800(2)	9.28531(14)
c/Å	12.8425(6)	18.5844(2)	17.2580(3)
α/°	105.191(4)	77.341(1)	90
β/°	90.312(4)	71.283(1)	91.1625(13)
γ/°	94.241(4)	74.890(1)	90
Volume/Å^3	1835.63(14)	4667.9(1)	2407.26(6)
Z	2	2	2
$D_{calc.}$ / g · cm^{-3}	1.575	1.527	1.418
μ/mm^{-1}	9.895	8.124	8.301
F(000)	885.3	2193.8	1072.0
Size/mm^3	0.263×0.129×0.121	0.405 × 0.165 × 0.098	0.187 × 0.147 × 0.07
Radiation type	CuK_α	CuK_β	CuK_α
Wavelength/Å	1.54184	1.39222	1.54178
2Θ range for data collection/°	7.44 to 133.28	5.94 to 144.52	5.884 to 145.746
Index ranges	-12 ≤ h ≤ 14, -11 ≤ k ≤ 14, -15 ≤ l ≤ 14	-20 ≤ h ≤ 19, -23 ≤ k ≤ 25, -25 ≤ l ≤ 20	-18 ≤ h ≤ 15, -6 ≤ k ≤ 11, -21 ≤ l ≤ 20
Refl. collected	19066	44596	9257
Independent Refl.	6421	23941	4670
R_{int}	0.0357	0.0226	0.0352
R_{sigma}	0.0372	0.0285	0.0431
Data/restraints/ parameters	6421/438/784	23941/0/911	4670/0/262
Goodness-of-fit on F^2	1.079	1.031	1.033
wR_2 (all data)	0.0604	0.0750	0.1222
wR_2	0.0579	0.0743	0.1155
R_1 (all data)	0.0322	0.0290	0.0502
R_1	0.0268	0.0280	0.0443
Largest Peak	0.48	0.86	0.81
Deepest Hole	-0.45	-0.89	-0.64

Table S8. Crystallographic data for compounds **7**-**9**.

Compound	**7**	**8**	**9**
CCDC-number	2479902	2479903	2479904
Formula	$C_{86}H_{156}O_{20}P_{20}K_8Fe_4$	$C_{34}H_{64}FeK_2O_{14.5}P_5$	$C_{36.4}H_{67.8}FeNa_2O_{11.6}P_5Te_2$
Formula Weight	2665.70	993.75	1202.98
Temperature/K	123(2)	123.00(10)	293(2)
Crystal System	monoclinic	monoclinic	monoclinic
Space Group	C2/c	$P2_1/c$	$P2_1/c$
a/Å	36.040(3)	13.3998(2)	13.5604(3)
b/Å	12.3893(6)	13.9227(2)	12.6495(2)
c/Å	34.165(2)	25.9090(4)	15.7331(4)
α/°	90	90	90
β/°	118.971(9)	104.266(2)	98.128(2)
γ/°	90	90	90
Volume/Å^3	13346.1(19)	4684.56(13)	2671.62(10)
Z	4	4	2
$D_{calc.}$ / g · cm^{-3}	1.327	1.409	1.495
μ/mm^{-1}	8.353	4.642	1.567
F(000)	5552.0	2092.0	1212.0
Size/mm^3	0.246 × 0.037 × 0.013	0.405 × 0.165 × 0.098	0.272 × 0.173 × 0.049
Radiation type	CuK_α	CuK_β	MoK_α
Wavelength/Å	1.54178	1.39222	0.71073
2Θ range for data collection/°	7.666 to 146.282	6.146 to 135.742	6.872 to 64.486
Index ranges	-44 ≤ h ≤ 39, -10 ≤ k ≤ 14, -41 ≤ l ≤ 41	-17 ≤ h ≤ 16, -18 ≤ k ≤ 18, -27 ≤ l ≤ 34	-17 ≤ h ≤ 19, -17 ≤ k ≤ 17, -21 ≤ l ≤ 23
Refl. collected	20971	23326	29024
Independent Refl.	12713	11184	16484
R_{int}	0.0595	0.0236	0.0196
R_{sigma}	0.0992	0.0318	0.0401
Data/restraints/ parameters	12713/64/670	11184/0/522	16484/709/749
Goodness-of-fit on F^2	0.865	1.028	1.053
wR_2 (all data)	0.1859	0.1343	0.1129
wR_2	0.1708	0.1262	0.1039
R_1 (all data)	0.1112	0.0571	0.0572
R_1	0.0670	0.0477	0.0438
Largest Peak	1.28	0.81	0.72
Deepest Hole	-0.74	-0.36	-0.84

Table S9. Crystallographic data for compounds **9'**.

Compound	**9'**
CCDC-number	2479905
Formula	$C_{56.63}H_{83.47}FeNa_2O_{12.05}P_6Te_2$
Formula Weight	1499.96
Temperature/K	293(2)
Crystal System	triclinic
Space Group	$P\bar{1}$
a/Å	12.8122(3)
b/Å	15.5393(4)
c/Å	19.0865(4)
α/°	80.520(2)
β/°	78.115(2)
γ/°	90
Volume/Å^3	87.576(2)
Z	2
$D_{calc.}$ / g · cm^{-3}	9.563
μ/mm^{-1}	8.353
F(000)	1523.0
Size/mm^3	0.265 × 0.198 × 0.104
Radiation type	CuK_α
Wavelength/Å	1.54184
2Θ range for data collection/°	7.05 to 145.884
Index ranges	-14 ≤ h ≤ 15, -17 ≤ k ≤ 19, -20 ≤ l ≤ 23
Refl. collected	40883
Independent Refl.	14221
R_{int}	0.0319
R_{sigma}	0.0308
Data/restraints/parameters	14221/1110/1008
Goodness-of-fit on F^2	1.038
wR_2 (all data)	0.0976
wR_2	0.0997
R_1 (all data)	0.0373
R_1	0.0351
Largest Peak	1.03
Deepest Hole	-0.54

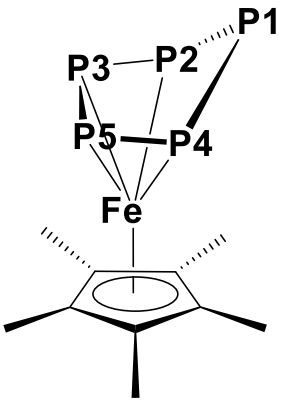

Table S10. Comparison of P-P and Fe−(P2P3P4P5)$_{centroid}$ distances in **B** and compounds **1**-**9'** in Å.

Compound	P1−P2	P1−P4	P2−P3	P4−P5	P3−P5	Fe−(P2P3P4P5)$_{centroid}$
B	2.1528(15)	2.1558(13)	2.2370(12)	2.2265(11)	2.1330(14)	1.5600(6)
1	2.1559(15)	2.1662(15)	2.1591(18)	2.156(2)	2.1292(19)	1.5648(8)
2	2.1670(8)	2.1511(4)	2.1515(11)	2.1497(9)	2.1239(13)	1.5674(4)
3	2.1771(7)-2.1834(7)	2.1849(7)-2.1850(11)	2.1360(9)-2.1361(10)	2.1430(11)--2.1462(7)	2.1737(8)-2.1738(10)	1.5692(4)-1.5726(5)
4	2.1784(9)	2.1782(8)	2.1273(10)	2.1468(10)	2.1683(10)	1.5697(5)
5	2.1787(5)-2.1856(5)	2.1809(5)-2.1860(7)	2.1368(5)-2.1406(6)	2.1386(5)-2.1445(6)	2.1647(5)-2.1656(5)	1.5603(3)-1.5606(4)
6	2.1349(11)	2.1355(10)	2.1415(13)	2.1271(12)	2.1424(14)	1.5577(6)
7	2.143(2)-2.171(14)	2.143(2)-2.171(3)	2.138(2)-2.143(3)	2.168(3)-2.172(8)	2.156(3)-2.172(3)	1.5658(15)-1.5800(14)
8	2.1974(7)	2.2109(10)	2.1175(10)	2.1264(9)	2.1905(12)	1.5702(6)
9	2.196(2)	2.180(2)	2.134(2)	2.130(2)	2.159(2)	1.5721(11)
9'	2.1875(9)	2.1911(10)	2.1353(11)	2.1404(11)	2.1576(10)	1.5665(6)

4. References:

[1] O. J. Scherer, T. Brück, *Angew. Chem.* **1987**, *99*, 59.

[2] M. V. Butovskiy, G. Balázs, M. Bodensteiner, E. V. Peresypkina, A. V. Virovets, J. Sutter, M. Scheer, *Angew. Chem. Int. Ed.* **2013**, *52*, 2972-2976.

[3] R. C. Clark, J. S. Reid, *Acta Cryst.* **1995**, *A51*, 887–897.

[4] G.M. Sheldrick, *Acta Cryst*. **2015**, *A71*, 3-8.

[5] G.M. Sheldrick, *Acta Cryst*. **2015**, *C71*, 3-8.

[6] L.J. Bourhis, O.V. Dolomanov, R.J. Gildea, J.A.K. Howard, H. Puschmann, *Acta Cryst.* **2015**, *A71*, 59-75.

[7] F. Kleemiss, O.V. Dolomanov, M. Bodensteiner, N. Peyerimhoff, L. Midgley, L.J. Bourhis, A. Genoni, L.A. Malaspina, D. Jayatilaka, J.L. Spencer, F. White, B. Grundkoetter-Stock, S. Steinhauer, D. Lentz, H. Puschmann, S. Grabowsky, *Chem. Sci*. **2021**, *12*, 1675-1692.

[8] O.V. Dolomanov, L.J. Bourhis, R.J. Gildea, J.A.K. Howard, H. Puschmann, *J. Appl. Cryst.* **2009**, *42*, 339-341